CrystEngComm

Accepted Manuscript

This article can be cited before page numbers have been issued, to do this please use: C. C. Seaton, R. R. Thomas, E. A. A. Essifaow, E. Nauha, T. Munshi and I. J. Scowen, *CrystEngComm*, 2018, DOI: 10.1039/C8CE00606G.

ROYAL SOCIETY OF CHEMISTRY

rsc.li/crystengcomm

View Article Online
DOI: 10.1039/C8CE00606G

Journal Name

ARTICLE

Structural Motifs in Salts of Sulfathiazole: Implications for Design of Salt Forms in Pharmaceuticals APIs

Received 00th January 20xx,
Accepted 00th January 20xx

DOI: 10.1039/x0xx00000x

www.rsc.org/

Colin C. Seaton*[a], Rayan R. Thomas[a], Eman A. A. Essifaow,[a] Elisa Nauha,[b] Tasnim Munshi[b], Ian J. Scowen*[b]

The creation of salts is a frequently used approach for the modification of physicochemical properties of an active pharmaceutical ingredient. Despite the frequency of application, there has been little research into the structural-property relationships of the final material and the nature of the counterion present. This work reports on five new salts of sulfathiazole and compares the energetics of the intermolecular interactions with variation in the crystal packing motifs.

Introduction

Altering the physicochemical properties of drug materials through manipulation of their solid-state forms has attracted considerable attention.[1] The creation of multi-component crystals (e.g. co-crystals, salts and solid solutions) is seen as a highly attractive and adaptable route for the modification of the physicochemical properties of active pharmaceutical ingredients (APIs)[2-4] resulting from structural and electrostatic factors. Both salts and co-crystals feature a new crystal structures with defined intermolecular interactions between the two (or more) components, while a solid solution retains the parent crystal structure of one component with the second randomly distributed throughout the crystal lattice. Salts differ from co-crystals in that pairs of oppositely charged molecular species are present and in the case of organic salts, this often corresponds to a single proton transfer within the crystal.

The creation of such materials is now common and, in several cases, the new phases have been shown alterations of properties such as solubility, stability and process performance (e.g. tableting).[5-10] Furthermore, utility of multi-component approaches has been demonstrated in cases using co-crystallisation as a purification step.[11,12] However, the design and selection of components and crystal forms is still often undertaken through trial and error or serendipitous study. Designing for a pre-defined change in physical properties, such as creating a new phase with a specific solubility, is still beyond the state of the art within the field. Many studies have focused on developing 'design' rules to predict how changes in molecular structure of the component can influence co-crystallisation.[13-16] It has been shown that successful formation may be predicted by consideration of the interactions between the components,[17] that the nature of the substituent groups can alter the ability to form co-crystals.[14,18] In contrast comparable studies for salt formers are more unusual and while proton transfer can related to both chemical and crystallographic structure in certain systems,[19]. few studies investigating the interaction between molecular structures, intermolecular interactions and formation have been presented. Systematic examples altering the counterions have been reported for ephedrine,[20-22] tyramine,[23] gemfibrozil, flurbiprofen, ibuprofen and etodolac salts[24] and studies into series of sulfonic acid salts have also emerged.[25] Unlike co-crystals, salts feature an additional set of unidirectional electrostatic interactions between the charged species (both repulsive and attractive) in addition to the crystal packing directing interactions. Understanding the balance between the numerous potential interactions is required to design such functional materials. Alteration of the key interactions between the components within a salt by, for example, changing the nature of the counterion (and its ability to hydrogen bond, form common motifs and intervene in the hydrogen patterns of the analogous molecular systems) will directly influence the lattice energy of the final phase and so the physicochemical properties of the new phase. Given the non-directional nature of electrostatic interactions, and their influence over long-ranges, investigating the relative importance of such interactions in the context of other intermolecular forces requires relatively sophisticated computational evaluations. Such approaches offer significant potential for insight into the assembly of salt-forms. Recently computational studies have indicated that the central role of directing hydrogen bonding in the analysis and design of organic materials has been overemphasised[26] and calculation of interaction energies between the molecular species is required to fully understand the assembly of the crystal structure.

[a] School of Chemistry and Biosciences, University of Bradford, Bradford, UK BD7 1DP. E-mail: c.seaton@bradford.ac.uk
[b] School of Chemistry, Joseph Banks Laboratories, University of Lincoln, Lincoln, UK, LN6 7TS. E-mail: iscowen@lincoln.ac.uk

Electronic Supplementary Information (ESI) available: Details of the crystal structure solution and refinement, crystal structure packing analysis of literature systems and crystal strucutres in cif format. See DOI: 10.1039/x0xx00000x

View Article Online
DOI: 10.1039/C8CE00606G

Sulfathiazole (STZ) is well established as a studied model active pharmaceutical ingredient (API) and its five polymorphic forms have been extensively considered.[27] There are a plethora of multi-component crystals formed including over one hundred solvates,[28] however, published crystal structures are only available for thirteen co-crystals (Table S2).‡ The molecule can undergo tautomerism and capable of forming salts with either acids or bases (Figure 1). Previous studies into STZ salts are also limited to four systems with STZ acting as a base and nine where it acts as an acid (Tables 1 and 2). This range of structural flexibility means that STZ offers an interesting material for further study to identify the role of different structural factors and intermolecular interactions on solid formation. To this end, salt formation between STZ and nitric acid (**I**), tetrafluoroboric acid (**II**), sulfuric acid (**III**), hydrochloric acid (**IV**), benzenesulfonic acid (**V**) and toluenesulfonic acid (**VI**) (Scheme 1) was investigated to identify how the crystal structure motifs are altered by variation of the components of the salt. The energetics of the new systems alongside those identified in the CSD were studied to identify the dominant interactions and how these potentially influence the lattice characteristics (energy and structure) of ionised components in these organic salts.

Table 1. Previously published STZ salts with acids.[§]

REFCODE	Chemical Structure
BUWDUT	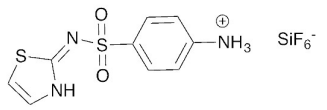
KUFWIT	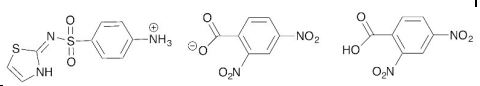
LOFMAW (polymorphic)	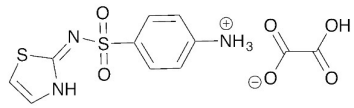
UDAKOA	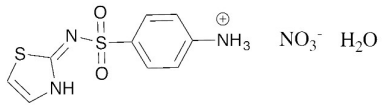

[§]Results from a CSD search as detailed before. Protonated and deprotonated forms of each tautomer were searched.

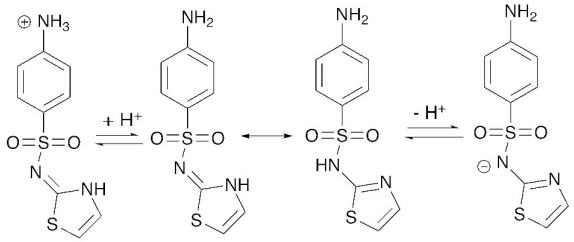

Figure 1. Molecular structures of STZ showing tautomerism and potential salt forms.

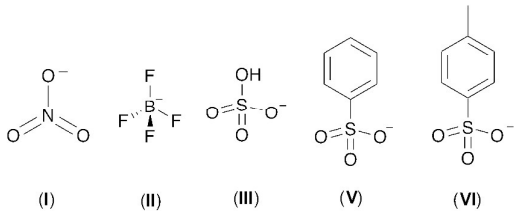

Scheme 1. Chemical structures of counterions used in this study.

View Article Online
DOI: 10.1039/C8CE00606G

Table 2. Previously published STZ salts with bases[§]

BUHMOI	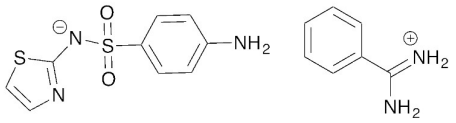
DOWPUC	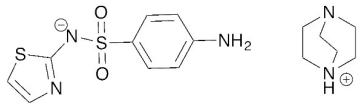
DOWQAJ	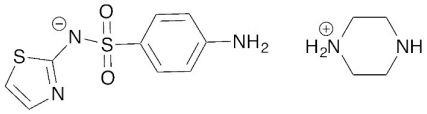
HSLSTZ	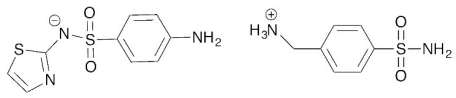
OHUWAR	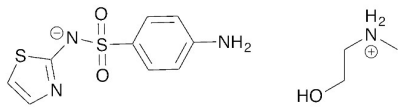
OHUWEV	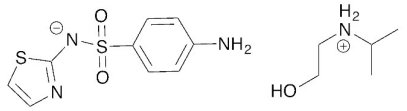
OHUWIZ	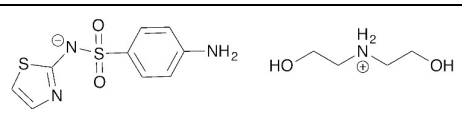
OEDWAZ	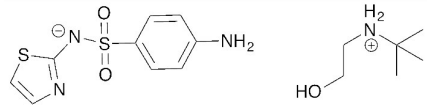
XIFPEI	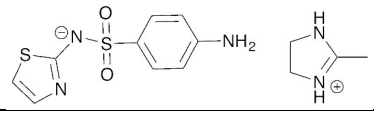

[§]Results from a CSD search as detailed before. Protonated and deprotonated forms of each tautomer were searched.

Methodology

Experimental

Crystallisation

Sulfathiazole salts were prepared by adding the appropriate acid (1 mmol) to a solution of sulfathiazole (1 mmol) in either methanol or acetone (4 cm^3). The solutions were filtered to obtain clear solutions and then slow evaporation of the solvent was allowed to promote crystal growth. Single crystals suitable for crystal structure analysis were obtained for **I**, **II**, **III**, **V** and **VI**, while PXRD on the powders obtained for **IV** indicated a new crystal phase, successful growth of suitable crystal was not achieved for **IV**.

Single Crystal Structure Determination

The crystallographic details for all systems are given in Table S1. The data was collected on a Bruker X8 Apex II diffractometer using graphite monochromated Mo Kα radiation at 173 K. The data was collected and reduced using Bruker SMART software. The structures of **I**, **II** and **III** were solved and refined using SHELXTL, whereas the structures of **V** and **VI** were solved and refined in Olex2[29] using SHELXT and SHELXL.[30] The structure of **VI** revealed the presence of a channel containing disordered solvent; this was modelled using squeeze methodology in Platon.[31] The resulting structure files have been deposited with Cambridge Crystallographic Data Centre (CCDC 1499236-1499240).

Computational

Lattice Energies

The hydrogen locations in all crystal structures were normalised and the lattice energies of resulting structures minimised using Forcite in the Materials Studio package. Given the wide range of atom types in the salts considered, a limited number of force fields were available for the energy calculations. Lattice energies were calculated using the Universal force field[32,33] with atomic point charges derived for each molecule by fitting to the electrostatic potential calculated from a DFT calculation (TPSS-D3/def2-TZVPPD)[34-36] in the program orca,[37] for all systems, while AA-CLP force field[38] was also used for selected systems. In this case, the crystal structures were optimised by downhill simplex method with fixed unit cell parameters. For **III**, **V** and **BUWDUT**, the disordered crystal structures were converted to ordered models in lower symmetries. In the case of **III** and **V**, the unit cells were initially reduced to P1 symmetry, half of the disordered components were removed and additional symmetry identified by ADDSYM program in Platon to give a Z' = 1 structure in $P2_1/c$ (**III**) and a Z' = 2 structure in $Pna2_1$ (**V**). For **BUWDUT**, half the disordered components were removed and the symmetry reduced to P -1.

Molecular Clusters

Dimers and higher molecular clusters were extracted from the relevant crystal structure and the hydrogen atom locations optimised in the program orca (TPSS-D3/TZV(d) (main group) TZV (hydrogen)).[39,40] The binding energies were then calculated at the TPSS-D3/def2-TZVPPD level of theory with the basis set superposition error corrected for by the counterpoise method of Boys and Bernardi.[41]

Results and Discussion

View Article Online
DOI: 10.1039/C8CE00606G

Crystal Structure Analysis

Salt **I** is shown to be a hydrogen nitrate salt (NO_3/HNO_3). The $STZH^+$ molecules link into a 1-D chain with a NO_3/HNO_3 pair bridging the two chains through NH…O bonds to forming a bilayer structure (Figure 2). These 2-D layers then link to form the final 3-D structure through weaker CH…O=S interactions.

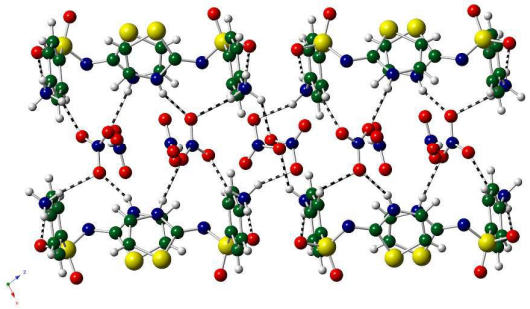

Figure 2. Formation of bilayer structure in **I** between $STZH^+$ and NO_3/HNO_3 ions.

Salt **II** forms a 1:1 salt with BF_4^-, which produces a 1-D chain between $STZH^+$ cations through N-H…N hydrogen bonds, with the BF_4^- anion bonding through N-H…F interactions to form a 2-D sheet structure (Figure 3). The final 3-D structure is formed through NH…O=S hydrogen bonds.

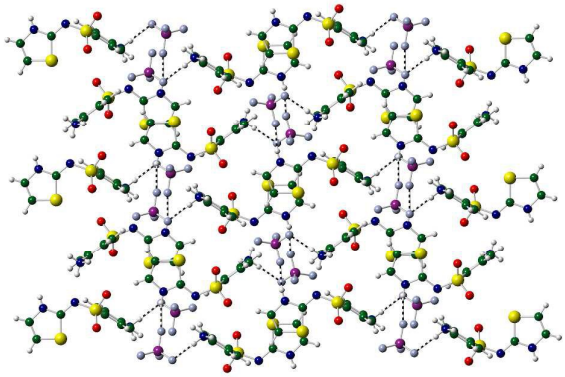

Figure 3. Formation of a 2-D sheet in **II** through NH…N and NH…F bonds.

The crystal structure of **III** indicates that two molecules of STZ, a single sulfate ion and an isolated oxygen atom present in the asymmetric cell. However, the disorder in the structure makes it hard to clearly identify all the hydrogen atoms and resolve the system as either HSO_4^-/OH^- or SO_4^{2-}/H_2O. The S-O bond lengths in the sulfate group are characteristic of a HSO_4^- anion (three ~1.45 Å and one ~1.55 Å). The distance from the isolated oxygen to the oxygen in the sulfate group is very short (1.8 Å) and so a central shared hydrogen present between the groups is possible. The crystal structure of **III** is isostructural to that of **BUWDUT**. The STZ cations hydrogen bond into a dimer through $^+$NH...N= hydrogen bonds, which then form a 1-D chain through NH...O hydrogen bonds with the HSO_4^-/OH^- cluster (Figure 4). The final 3-D structure is constructed through the interlinking of these chains.

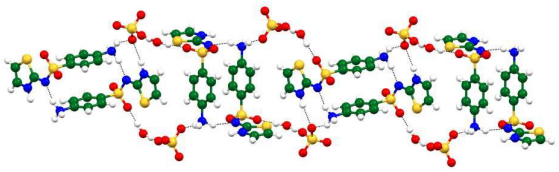

Figure 4. Formation of a 1-D chain between STZ/HSO_4^-/OH^- groups in **III**.

Salt **V** formed with benzenesulfonate has a 1:1 composition and the crystal structure displays an orientation disorder in the aromatic component with a 50:50% split. The two components are hydrogen bonded together through NH...O=S hydrogen bonds to form two ring motifs, one a $R^4_4(12)$ motif formed by two benzenesulfonate SO_3 groups bridging two NH_3^+ group on STZ (Figure 5a), while the second is a $R^4_4(28)$ motif which binds four molecules through N_{ring}-H...O=S and NH_3^+...O=S bonds (Figure 5b). The combination of these motifs form a 2-D sheet structure in the crystal, which are packed into the final 3-D structure through CH…O=S interactions.

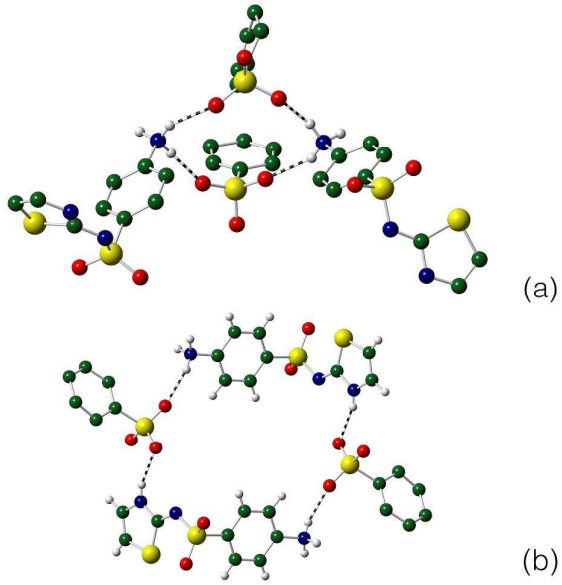

Figure 5. Formation of tetramers in the crystal structure of **V**, (a) $R^4_4(12)$ motif and (b) $R^4_4(28)$ motif. Only one component of disordered benzenesulfonate counterion is shown and selected hydrogens removed for clarity.

Crystal structure determination of **VI** confirmed that STZ had undergone an acid catalysed aldol reaction with the acetone solvent (Scheme 2). The resulting product forms a salt with the toluenesulfonic acid. Attempts to crystallise from other solvents resulted in poor quality crystals and attempts to determine a structure for STZ with toluenesulfonate were unsuccessful. Strong $^+$NH...$^-$O=S hydrogen bonds between the two components of the salt, forms a 1-D channel which is filled with disordered solvent (Figure 6). The channel void space is calculated to be 277 $Å^3$ (10% of unit cell volume) and runs through the entire crystal structure along the *b*-axis. These channels are linked through weaker CH…O bonds to construct the final crystal structure.

View Article Online
DOI: 10.1039/C8CE00606G

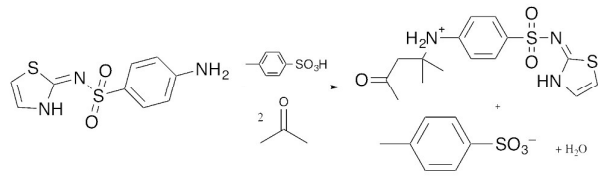

Scheme 2. Formation of aldol product (**VI**) with sulfathiazole and toluenesulfonic acid.

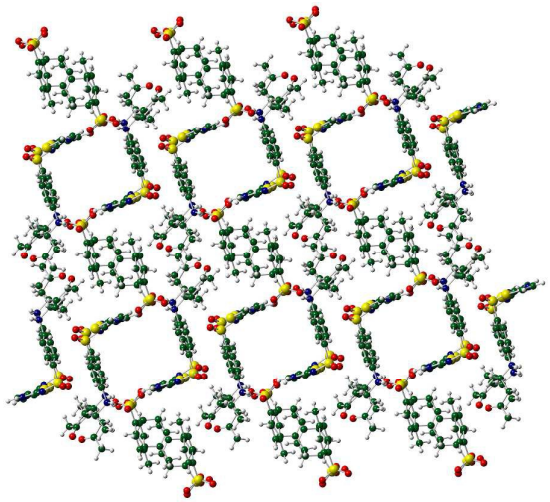

Figure 6. Formation of channel structure in **VI**.

Comparison of crystal structures

Analysis of the crystal packing of the structures present in the CSD is given in the electronic supplementary information. While all the known STZ polymorphs form dimers between the STZ molecules, dimer formation only occurs in three salts (**BUWDUT**, **KUFWIT** and **III**) that display different hydrogen bonding to each other and the polymorphs. While a repulsion between the positively charged STZ ions would be expected, the relative isolation of the charged species at one end of the relative large component the sum of other interactions may be larger enough to overcome the repulsion. Thus, the interaction energies were quantified for the various crystals and molecular components.

Computational Studies

Lattice energies for the STZ salts were calculated using two force fields (Table 3) that give different ordering of the crystal structures. However, in both cases the lowest energy systems are those systems with the largest charge on a single counterion (SiF_6^{2-} and SO_4^{2-}). Alteration of the hydrogen location for **III** (from SO_4^{2-} to HSO_4^-) alters the absolute energy of the system but not the relative position in either list. Both these structures are isostructural and so geometrical and electrostatic interactions appear to be dominant in this case. The systems with specific hydrogen bonds between the components have lower lattice energies suggesting that complementary design of hydrogen bonding with electrostatic and geometric factors could be a key factor in the creation of high stability phases.

Table 3. Calculated Lattice Energies of STZ salts (sorted by AA-CLP energies)

System	Universal Force Field Lattice Energy (kJ·mol^{-1})	AA-CLP Lattice Energy (kJ·mol^{-1})
BUWDUT (SiF_6^{2-})	-917.57	-739.73
III (SO_4^{2-}/H_2O)	-765.86	-523.15
III (HSO_4^-/OH^-)	-444.8	-484.25
V (benzenesulfonate)	-232.23	-417.65
I (NO_3^-/HNO_3)	-165.03	-403.11
KUFWIT (2,4-dinitrobenzoate/2,4-dinitrobenzoic acid)	-544.1	-288.562
LOFMAW (hydrogen oxalate)	-579.1	-254.372
LOFMAW01 (hydrogen oxalate)	-517.15	-239.478
UDAKOA (NO_3^-/H_2O)	-209.58	-209.97
II (BF_4^-)	-313.69	-184.91

Molecular Dimers

The energies of closest pairs of $STZH^+$/$STZH^+$, $STZH^+$/anion and anion/anion ions from each crystal structure were calculated for the geometry in the crystal structure (Table 4, Figures 7, 8, 9). As expected the electrostatic contribution dominates the energetics, with attractive forces between the anion and cation and repulsive forces in the cation/cation and anion/anion pairs. Dimers between $STZH^+$ ions are present in **III**, **BUWDUT** and **KUFWIT**. In **III** and **BUWDUT** are linked through two NH…N hydrogen bonds, while **KUFWIT** utilises two NH…O=S bonds. In both cases the energy gained by the interactions offsets the repulsive energy of the electrostatic interaction within the dimer. However, during the hydrogen location optimisation for **III** cation/anion pair, significant rearrangement of the hydrogen atoms took place resulting in a neutral STZ molecule, which gives a significantly lower energy. The remaining systems have a single hydrogen bond between the $STZH^+$ ions forming a 1-D chain motif in each case; this does not shield repulsive interaction as effectively. The difference in binding energy for the two polymorphs of the oxalate appears to be driven by the different conformations of the oxalate anion. In form I, an intramolecular hydrogen bond stabilises that form by 41.33 kJ·mol^{-1}.

View Article Online
DOI: 10.1039/C8CE00606G

Table 4. Binding Energies of Key Motifs in STZ salts crystal structures

System	$STZH^+$/Anion Energy ($kJ{\cdot}mol^{-1}$)	$STZH^+$/$STZH^+$ Energy ($kJ{\cdot}mol^{-1}$)	Anion/Anion Energy ($kJ{\cdot}mol^{-1}$)
BUWDUT (SiF_6^{2-})	-700.17	45.72	964.05
LOFMAW01 (hydrogen oxalate)	-462.85	154.25	156.30
UDAKOA (NO_3^-/H_2O)	-434.76	121.34	252.72
II (BF_4^-)	-430.83	110.98	313.56
I (NO_3^-/HNO_3)	-362.81	115.28	343.08
V (benzenesulfonate)	-289.98	107.22	422.25
LOFMAW (hydrogen oxalate)	-250.80	125.82	221.86
KUFWIT (2,4-dinitrobenzoate)	-203.88	5.91	229.05
III (HSO_4/H_2O)*	-94.37	57.86	939.97

*After hydrogen position optimisation, the cation…anion system had rearranged to give a trimer with a HSO_4, H_2O and a neutral STZ. Anion pairs calculated for SO_4^{2-} system.

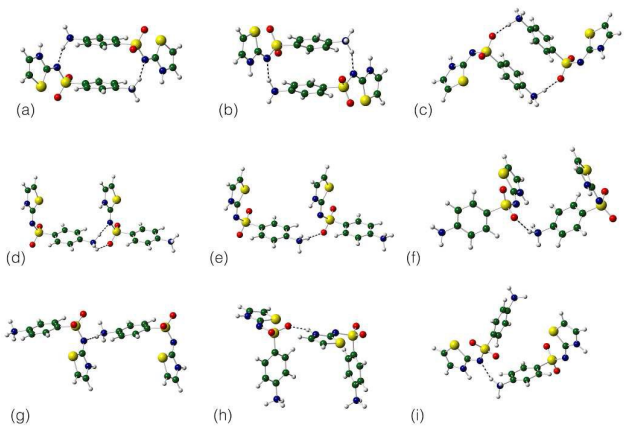

Figure 7. Hydrogen position optimised $STZH^+/STZ^+$ dimers in (a) BUWDUT, (b) **III**, (c) KUFWIT (d) **V**, (e) **I**, (f) UDAKOA, (g) LOFMAW, (h) LOFMAW01 and (i) **II**.

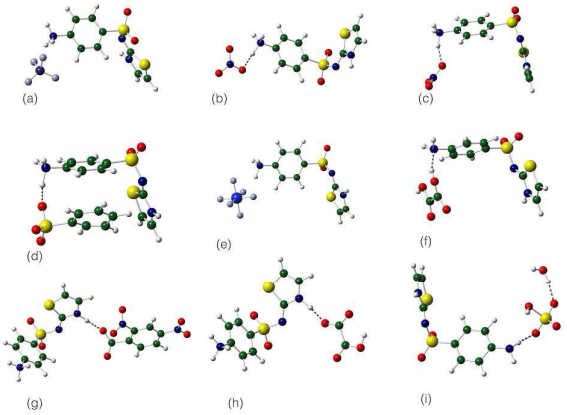

Figure 8. Hydrogen position optimised anion/STZ dimers in (a) **II**, (b) UDAKOA, (c) **I**, (d) **V**, (e) BUWDUT, (f) LOFMAW01, (g) KUFWIT, (h) LOFMAW and (i) **III**.

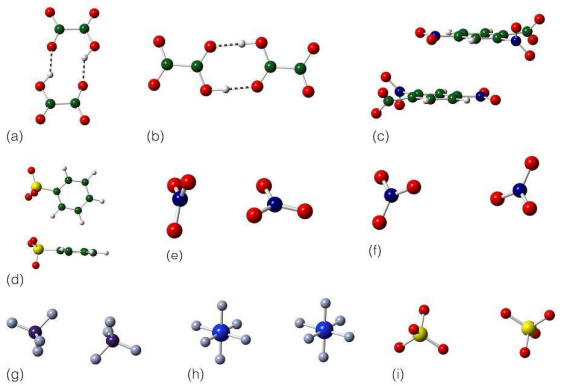

Figure 9. Hydrogen position optimised anion/anion pairs in (a) LOFMAW, (b) LOFMAW01, (c) KUFWIT, (d) **V**, (e) UDAKOA, (f) **I**, (g) **II**, (h) BUWDUT and (i) **III**.

The polymorphs of pure STZ display dimers in forms I - IV and a tetramer in form V. The hydrogen bonding in form I differs from forms II - IV as it contains a $R^2_2(8)$ motif formed by NH…N bonds, while the other, has a mix of NH…N and NH…O=S bonds (Figure 10). The mixed H-bond motif is the lowest energy (Table 5), however it is present in the stable phases of STZ and is not similar to the motifs present in the salts determined. Importantly, these H-bonded motifs all correspond with attractive STZ…STZ interaction in the lattice.

Table 5. Energies for STZ Polymorphs key motifs.

Polymorph	STZ…STZ Energy ($kJ{\cdot}mol^{-1}$)	Energy per molecule ($kJ{\cdot}mol^{-1}$)
Form I dimer	-109.42	-54.71
Form II/III/IV dimer	-41.49	-20.75
Form V tetramer	-143.29	-35.82

View Article Online
DOI: 10.1039/C8CE00606G

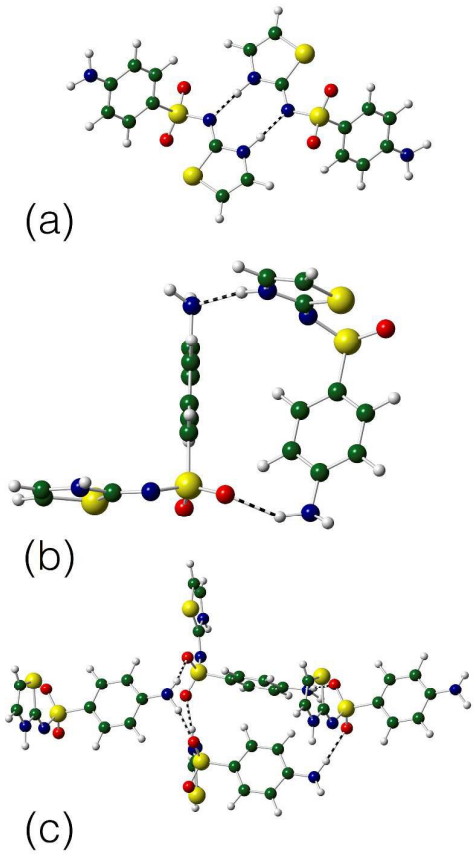

Figure 10. Comparison of the molecular motifs in (a) form I, (b) forms II - IV and (c) form V STZ.

As expected, the STZ…STZ interactions in the salts change to repulsive in the crystal lattice (Table 2). Three distinct groupings arise from considering the repulsions: (i) <50 kJ mol^{-1} [**III**, BEWDUT and KUFWIT], (ii) 100-125 kJ mol^{-1} [**I, II, V**, UDAKOA, LOFMAW], (iii) >150 kJ mol^{-1} [LOFMAW01]. It might be helpful in this context to view the salts as arrays of repulsive cations, whose repulsive interactions are mediated by the counterions. Broadly, it appears that interactions between the anion centres and the protonated amine (the centre of cationic charge), exerts a considerable influence in mediating the STZ…STZ repulsion. Intriguingly, these correlate with the relative dispositions of the protonated aniline centre of adjacent STZH$^+$ units in the crystal structure and the numbers of anions in the local vicinity: for grouping (i), the STZH$^+$ systems are arranged in a head-to-tail orientation an each have *two* anions in close contact with each anilinyl (-NH$_3^+$) centre - the remaining interaction to S=O and/or S-N of an adjacent STZH$^+$. For group (ii), the layered structures have a STZH$^+$ system in a head-to-tail orientation, but only one close contact with the counterion is observed (again remaining interactions at the NH$_3^+$ arise from S=O / S-N or HN). For (iii), the LOFMAW01 outlier has close contacts to an oxH…oxH centrosymmetric dimer that brings the adjacent STZH$^+$ molecules together in a 'head to-head' orientation. Overall, it appears that increasing the number of anions surrounding the cation centre and their charge density effectively screens the repulsion between adjacent cations. Clearly this repulsion is maximised in the 'head-to-head' configuration. Similarly, the converse also appears to be true. Bringing charge dense anion centres into close proximity (**III** and BUWDUT), causes very large relative anion anion repulsions in excess of 600 kJ mol^{-1} compared to the more distal anions. While such 'charge-balance' concepts may prove valuable in unpicking the relative influences, it is the interplay of the relative cation-anion attractions, and cation-cation/anion-anion repulsions that dominate in the overall determination of the lattice energy. Importantly, H-bonded motifs may considerably have less influence in ionised systems in the solid state.

Conclusions

These studies have established an important approach to understanding the relative importance of intermolecular interactions in salts of pharmaceutical products, through a combination of systematic experimentation (complimenting database structures) and computational analysis of the lattice energies of the resulting crystal structures. It appears from this study that converting molecular species with potential to form diverse hydrogen bonding motifs in the solid to their analogous salt forms switches the intermolecular interaction from attraction to overall repulsion. Furthermore, the mediation of repulsion between charged centres with judicious choice of anion to 'screen' the repulsions between adjacent molecules, offers a route to influence lattice energy and hence the crystal packing of pharmaceutical ingredients.

Notes and references

‡ Cambridge structure database (CSD) version 5.37 with 3 updates was searched using Conquest 1.18 for systems containing either tautomer. Only organic systems were included.

1 N. Blagden, M. de Matas, P. T. Gavan and P. York, *Adv. Drug Del. Rev.*, 2007, **59**, 617–630.
2 I. Miroshnyk, S. Mirza and N. Sandlert, *Expert Opin. Drug Del.*, 2009, **6**, 333–341.
3 R. Thakuria, A. Delori, W. Jones, M. P. Lipert, L. Roy and N. Rodriguez-Hornedo, *Int. J. Pharm.*, 2013, **453**, 101–125.
4 Ö. Almarsson and M. J. Zaworotko, *Chem. Commun.*, 2004, 1889–1896.
5 A. V. Trask, W. D. S. Motherwell and W. Jones, *Cryst. Growth Des.*, 2005, **5**, 1013–1021.
6 S. Karki, T. Friščić, L. Fábián, P. R. Laity, G. M. Day and W. Jones, *Adv. Mater.*, 2009, **21**, 3905–3909.
7 H. D. Williams, N. L. Trevaskis, S. A. Charman, R. M. Shanker, W. N. Charman, C. W. Pouton and C. J. H. Porter, *Pharmacol. Rev.*, 2012, **65**, 315–499.
8 D. R. Weyna, M. L. Cheney, N. Shan, M. Hanna, M. J. Zaworotko, V. Sava, S. Song and J. R. Sanchez-Ramos, *Mol. Pharmaceutics*, 2012, **9**, 2094–2102.
9 C. B. Aakeröy, *Acta Crystallogr., Sect. B Struct. Sci. Cryst. Eng. Mater.*, 2015, 1–5.
10 G. Bolla and A. Nangia, *Chem. Commun.*, 2016, **52**, 8342–8360.

View Article Online
DOI: 10.1039/C8CE00606G

11 A. Delori, T. Friščić and W. Jones, *CrystEngComm*, 2012, **14**, 2350.
12 P. Billot, P. Hosek and M.-A. Perrin, *Org. Process Res. Dev.*, 2013, **17**, 505–511.
13 G. R. Desiraju, *J. Am. Chem. Soc.*, 2013, **135**, 9952–9967.
14 C. C. Seaton, *CrystEngComm*, 2011, **13**, 6583–6595.
15 C. B. Aakeröy and D. J. Salmon, *CrystEngComm*, 2005, **7**, 439–448.
16 T. Friščić and W. Jones, *Cryst. Growth Des.*, 2009, **9**, 1621–1637.
17 D. Musumeci, C. A. Hunter, R. Prohens, S. Scuderi and J. F. McCabe, *Chem. Sci.*, 2011, **2**, 883–890.
18 C. C. Seaton, K. Chadwick, G. Sadiq, K. Guo and R. J. Davey, *Cryst. Growth Des.*, 2010, **10**, 726–733.
19 C. C. Seaton, *CrystEngComm*, 2014, **16**, 5878–5886.
20 E. A. Collier, R. J. Davey, S. N. Black and R. J. Roberts, *Acta Crystallogr., Sect. B: Struct. Sci.*, 2006, **62**, 498–505.
21 S. N. Black, E. A. Collier, R. J. Davey and R. J. Roberts, *J. Pharm. Sci.*, 2007, **96**, 1053–1068.
22 C. L. Cooke, R. J. Davey, S. N. Black, C. Muryn and R. G. Pritchard, *Cryst. Growth Des.*, 2010, **10**, 5270–5278.
23 N. E. B. Briggs, A. R. Kennedy and C. A. Morrison, *Acta Crystallogr., Sect. B: Struct. Sci.*, 2012, **68**, 453–464.
24 S. E. David, P. Timmins and B. R. Conway, *Drug Dev. Ind. Pharm.*, 2012, **38**, 93–103.
25 D. P. Elder, E. Delaney, A. Teasdale, S. Eyley, V. D. Reif, K. Jacq, K. L. Facchine, R. S. Oestrich, P. Sandra and F. David, *J. Pharm. Sci.*, 2010, **99**, 2948–2961.
26 A. Gavezzotti, *CrystEngComm*, 2013, **15**, 4027–4035.
27 A. Munroe, Å. C. Rasmuson, B. K. Hodnett and D. M. Croker, *Cryst. Growth Des.*, 2012, **12**, 2825–2835.
28 A. L. Bingham, D. S. Hughes, M. B. Hursthouse, R. W. Lancaster, S. Tavener and T. L. Threlfall, *Chem. Commun.*, 2001, 603–604.
29 O. V. Dolomanov, L. J. Bourhis, R. J. Gildea, J. A. K. Howard and H. Puschmann, *J. Appl. Cryst.*, 2009, **42**, 339–341.
30 G. M. Sheldrick, *Acta Crystallogr., Sect. A: Found. Crystallogr.*, 2008, **64**, 112–122.
31 A. L. Spek, *Acta Crystallogr., Sect. C Struct. Chem.*, 2015, **71**, 9–18.
32 C. Casewit, K. Colwell and A. Rappe, *J. Am. Chem. Soc.*, 1992, **114**, 10035–10046.
33 C. Casewit, K. Colwell and A. Rappe, *J. Am. Chem. Soc.*, 1992, **114**, 10046–10053.
34 D. Rappoport and F. Furche, *J. Chem. Phys.*, 2010, **133**, 134105.
35 S. Grimme, J. Antony, S. Ehrlich and H. Krieg, *J. Chem. Phys.*, 2010, **132**, 154104.
36 S. Grimme, S. Ehrlich and L. Goerigk, *J. Comput. Chem.*, 2011, **32**, 1456–1465.
37 F. Neese, *WIREs Comput. Mol. Sci.*, 2012, **2**, 73–78.
38 A. Gavezzotti, *New J. Chem.*, 2011, **35**, 1360–1368.
39 A. Schaefer, H. Horn and R. Ahlrichs, *J. Chem. Phys.*, 1992, **97**, 2571.
40 F. Weigend and R. Ahlrichs, *Phys. Chem. Chem. Phys.*, 2005, **7**, 3297.
41 S. Boys and F. Bernardi, *Mol. Phys.*, 1970, **19**, 553–566.